

Central Lancashire Online Knowledge (CLoK)

Title	Lactate Protects Microglia and Neurons from Oxygen-Glucose
	Deprivation/Reoxygenation
Type	Article
URL	https://clok.uclan.ac.uk/id/eprint/51079/
DOI	https://doi.org/10.1007/s11064-024-04135-7
Date	2024
Citation	Tassinari, Isadora D'Ávila, Rodrigues, Fernanda da Silva, Bertram, Craig, Mendes-da-Cruz, Daniella Arêas, Guedes, Renata Padilha, Paz, Ana Helena, Bambini-Junior, Victorio and de Fraga, Luciano Stürmer (2024) Lactate Protects Microglia and Neurons from Oxygen-Glucose Deprivation/Reoxygenation. Neurochemical Research, 49. pp. 1762-1781. ISSN 0364-3190
Creators	Tassinari, Isadora D'Ávila, Rodrigues, Fernanda da Silva, Bertram, Craig, Mendes-da-Cruz, Daniella Arêas, Guedes, Renata Padilha, Paz, Ana Helena, Bambini-Junior, Victorio and de Fraga, Luciano Stürmer

It is advisable to refer to the publisher's version if you intend to cite from the work. https://doi.org/10.1007/s11064-024-04135-7

For information about Research at UCLan please go to http://www.uclan.ac.uk/research/

All outputs in CLoK are protected by Intellectual Property Rights law, including Copyright law. Copyright, IPR and Moral Rights for the works on this site are retained by the individual authors and/or other copyright owners. Terms and conditions for use of this material are defined in the http://clok.uclan.ac.uk/policies/

Lactate protects microglia and neurons from oxygen-glucose deprivation/reoxygenation

Isadora D'Ávila Tassinari^{1,4}, Fernanda da Silva Rodrigues^{2,4}, Craig Bertram⁵, Daniella Arêas Mendes-da-Cruz^{3,4}, Renata Padilha Guedes², Ana Helena Paz¹, Victorio Bambini-Junior^{4,†}, Luciano Stürmer de Fraga^{1,†,*}

¹Graduate Program in Physiology, Institute of Basic Health Sciences (ICBS), Federal University of Rio Grande do Sul (UFRGS), Porto Alegre, 90050-003, Brazil.

²Graduate Program in Biosciences, Federal University of Health Sciences of Porto Alegre (UFCSPA), Porto Alegre, 90050-170, Brazil.

³Laboratory on Thymus Research, Oswaldo Cruz Institute, Oswaldo Cruz Foundation, Rio de Janeiro, 21040-360, Brazil.

⁴Division of Biomedical and Life Sciences, Faculty of Health and Medicine, Lancaster University, Lancaster, LA1 4YW, United Kingdom.

⁵School of Pharmacy and Biomedical Sciences, University of Central Lancashire, Preston, PR1 2HE, United Kingdom.

*Corresponding author. E-mail(s): lucianof@ufrgs.br; † These authors contributed equally to this work.

IDT: https://orcid.org/0000-0002-7745-6423
FSR: https://orcid.org/0000-0002-1070-6379
CB: https://orcid.org/0000-0002-3211-4585

DAMC: https://orcid.org/0000-0003-3697-1506
RPG: https://orcid.org/0000-0003-3668-767X
AHP: https://orcid.org/0000-0002-8590-6770
USF: https://orcid.org/0000-0001-7203-3467

Acknowledgements:

We want to express our gratitude to Dr. Amanda Thomaz from the Division of Biomedical and Life Sciences, Lancaster University, and also the PhD student, Janaína Zang from the Federal University of Rio Grande do Sul (UFRGS) for their unwavering support in the immunofluorescence experiments.

Abbreviations:

3,5-DHBA: 3,5-dihydroxybenzoic acid 4-CIN: α-Cyano-4-hydroxycinnamic acid

ANLSH: Astrocyte-neuron lactate shuttle hypothesis

ATP: Adenosine triphosphate

BCECF-AM: Acetoxymethyl ester of 2',7'-bis-(2-carboxyethyl)-5-(and-6)-carboxyfluorescein

cAMP: Cyclic adenosine monophosphate

CD206: Cluster of differentiation 206, mannose receptor

1

DAPI: 4',6-diamidino-2-phenylindole

DMEM: Dulbecco's Modified Eagle Medium ELISA: Enzyme-linked immunosorbent assay

FBS: Fetal bovine serum

GPR81: G protein-coupled-receptor 81

HCAR1: Hydroxy-carboxylic acid receptor 1

HCl: Hydrochloric acid

HEPES: 4-(2-hydroxyethyl)-1-piperazineethanesulfonic acid

HIF-1α: Hypoxia Inducible Factor 1 Subunit Alpha

OGD: Oxygen and glucose deprivation

OGD/R: Oxygen and glucose deprivation-reoxygenation

MCT: Monocarboxylate transporter

MTT: 3-(4,5-dimethylthiazol-2-yl)-2,5-diphenyltetrazolium bromide

NAD+: Nicotinamide adenine dinucleotide, oxidized form NADH: Nicotinamide adenine dinucleotide, reduced form

NEFL: Neurofilament light polypeptide

NF-κB: nuclear factor kappa B

NLRP3: Nod-like receptor protein 3

pHi: Intracellular potential of hydrogen

P/S: Penicillin/streptomycin PBS: Phosphate-buffer saline

PKA: protein kinase A

RA: Retinoic acid

RT: Room temperature

TNF-α: Tumor necrosis factor-alpha

Abstract

Lactate has received attention as a potential therapeutic intervention for brain diseases, particularly those including energy deficit, exacerbated inflammation, and disrupted redox status, such as cerebral ischemia. However, lactate roles in metabolic or signaling pathways in neural cells remain elusive in the hypoxic and ischemic contexts. Here, we tested the effects of lactate on the survival of a microglial (BV-2) and a neuronal (SH-SY5Y) cell lines during oxygen and glucose deprivation (OGD) or OGD followed by reoxygenation (OGD/R). Lactate signaling was studied by using 3,5-DHBA, an exogenous agonist of lactate receptor GPR81. Inhibition of lactate dehydrogenase (LDH) or monocarboxylate transporters (MCT), using oxamate or 4-CIN, respectively, was performed to evaluate the impact of lactate metabolization and transport on cell viability. The OGD lasted 6 h and the reoxygenation lasted 24h following OGD (OGD/R). Cell viability, extracellular lactate concentrations, microglial intracellular pH and TNF-a release, and neurite elongation were evaluated. Lactate or 3,5-DHBA treatment during OGD increased microglial survival during

reoxygenation. Inhibition of lactate metabolism and transport impaired microglial and neuronal viability. OGD led to intracellular acidification in BV-2 cells, and reoxygenation increased the release of TNF- α , which was reverted by lactate and 3,5-DHBA treatment. Our results suggest that lactate plays a dual role in OGD, acting as a metabolic and a signaling molecule in BV-2 and SH-SY5Y cells. Lactate metabolism and transport are vital for cell survival during OGD. Moreover, lactate treatment and GPR81 activation during OGD promote long-term adaptations that potentially protect cells against secondary cell death during reoxygenation.

Keywords: oxygen and glucose deprivation, lactate, microglia, neuron, metabolism

Introduction

For long considered a waste byproduct of metabolism, lactate is now used as an effective therapy for the harmful effects of energy deficits and to improve long-term outcomes in conditions such as cerebral ischemia [1–4]. Cerebral ischemia involves oxygen deprivation and ATP depletion, which impairs the ability of cells to maintain ion gradients, causing cell injury and death [5, 6]. Animal models of brain ischemia have focused on protective strategies to identify potential therapies for ischemic injury [7–9]. However, *in vitro* models – such as oxygen and glucose deprivation (OGD) in cell cultures – enable us to explore the underlying mechanisms in detail.

Lactate is the end-product of glycolysis and a vital exchange currency between glycolytic and oxidative cells to meet energetic demands. Exogenous lactate can be used as a metabolic substrate in energy-depleted conditions [4, 10, 11]. It has been postulated that metabolism and transport of lactate are required for these effects [12–14]. Cells can import or export lactate [15, 16] through monocarboxylate transporters (MCT), although their pattern of expression varies according to the cell type, environment and cell requirements [17, 18]. Neurons take advantage of the high-affinity MCT2 isoform for lactate uptake [19–21] and of the expression of lactate dehydrogenase 1 (LDH1) isoform to meet the energetic demands through lactate oxidation to pyruvate[22–24]; Astrocytes - cells with a more glycolytic profile - express the low-affinity MCT4 isoform [20, 25] which favors lactate export following synthesis through the LDH5 isoform [22–24], as proposed by the well-known and supported astrocyte-neuron lactate shuttle (ANLS) hypothesis [22, 26]. Microglia express MCT with particular isoforms influenced by metabolic status [15, 17]. How lactate shapes such responses in microglial cells remains to be discovered. Since neural responses to metabolic stress are cell-specific [27] and microglia are the main players in the primary CNS inflammatory responses [28–30] it is crucial to explore effects of lactate in such cells individually following oxygen-glucose deprivation.

Besides its metabolic function, lactate may be also beneficial due to anti-inflammatory signaling properties related to hydroxycarboxylic acid receptor 1 (HCAR1), also known as G protein-coupled-receptor 81 (GPR81) [31, 32]. The initial suggestions of an anti-inflammatory/signaling property of lactate were found in the LPS-induced acute pancreatitis and hepatitis model: lactate-treated macrophages presented a decrease in interleukin 1 beta (IL-1β) release and NLRP3 inflammasome activity, both dependent on GPR81 activation [33]. In recent years, GPR81's role in the central nervous system (CNS) has attracted substantial attention [34–37] in an attempt to describe the downstream cascade and the effects of receptor activation in different pathophysiological contexts affecting the brain. Other than lactate, 3,5-dihydroxybenzoic acid (3,5-DHBA) - a component present in most dietary traditions, which behaves as a GPR81 agonist - seems to exert beneficial effects in different CNS conditions by improving glucose metabolism, mitochondrial function, synaptic potentiation, and memory consolidation [36, 38–40]. However, there are also conflicting reports in the literature, implying that the pattern of responses following GPR81 activation depends on the cell type and environment [36, 41, 42], while some studies attribute microglial GPR81 as responsible for promoting resolutive inflammatory responses [43, 44].

As lactate is a molecule with many (possibly conflicting) roles, it is essential to investigate and distinguish its specific effects on metabolic and neuroimmune responses. Here, we investigate whether lactate affects microglial and neuronal survival in conditions of OGD or OGD/R. In the first set of experiments, we treated BV-2 microglial or SH-SY5Y neuronal cell lineages with lactate during OGD to verify whether lactate could be an effective substitute

for glucose and reduce neuronal death and pro-inflammatory microglial responses. As cerebral hypoxic-ischemic conditions *in vivo* are usually followed by a period of reoxygenation and later neuroinflammation, in the second set of experiments, BV-2 or SH-SY5Y cells also receiving lactate during OGD were submitted to a following period of reoxygenation (OGD/R). This allows to check if lactate administered to the cultures during OGD causes long-term changes - possibly *via* GPR81 - that improve BV-2 or SH-SY5Y survival even when cells were evaluated in the reoxygenation phase. To further elucidate the mechanism underlying the effects of lactate we also explored its putative signaling role using a GPR81 agonist and the impact of lactate metabolization and transport by inhibition of LDH and MCT, respectively.

Methods

Cell culture

BV-2 cells (RRID:CVCL_0182, provided by Dr. Vinicius Frias, IOC-Oswaldo Cruz Foundation) were cultured in Dulbecco's Modified Eagle Medium (DMEM) (DMEM GlutaMAXTM, #Cat: 31966047, ThermoFisher Scientific), supplemented with 10% fetal bovine serum (FBS) (#Cat: A5256701 Thermo Fisher Scientific) and 1% penicillin/streptomycin (P/S) (#Cat: 15140122, Thermo Fisher Scientific). SH-SY5Y cells (RRID:CVCL_0019, provided by Dr. Ed Parkin, Division of Biomedical and Life Sciences, Lancaster University) were cultured in DMEM/F12 (1:1) (DMEM #Cat: 11965092; F-12/Nutrient Mixture, #Cat: 11320033), supplemented with 10% FBS and 1% P/S. Cells were cultured at a density of 1 x 10⁵ cells/ml in T75 flasks and placed in a humidified incubator at 37°C in the presence of 5% CO₂ in the air until 80% confluence was achieved.

SH-SY5Y differentiation

SH-SY5Y cells were plated in DMEM/F12 (1:1), supplemented with 10% FBS and 1% P/S at a density of 1.5×10^3 cells/100 µL/well (96-well plate) and 5×10^4 cells/mL/well (12-well plate) overnight. The next day, differentiation day 1, the plates were centrifuged (233 x g, 5 minutes). The cell medium was replaced with differentiation media: NeurobasalTM Medium supplemented with 1% B-27TM (#Cat: 17504044, Thermo Fisher Scientific), 1% GlutaMAXTM (#Cat: 35050061, Thermo Fisher Scientific), and 1% P/S. Immediately before the media change, retinoic acid (RA) to a final concentration of 10 µM was added into the differentiation media. This media replacement was repeated on the differentiation days 4 and 7 to produce the three RA pulses. On day 8, the experiments using SH-SY5Y cells were performed.

Oxygen-glucose deprivation (OGD) and OGD/reoxygenation (OGD/R)

BV-2 cells were seeded the day before the OGD procedure in 96-well plates ($2x10^4$ cells/100 µL/well) or 12-well plates (10^5 cells /1 mL/well) to promote cell attachment. SH-SY5Y cells were seeded eight days before the OGD procedure, either in 96-well plates ($1.5x10^3$ cells/100 µL/well) or in 12-well-plates ($5x10^4$ cells/1 mL/well) to allow the differentiation of neuroblastoma SH-SY5Y cells into neuron-like cells. To simulate hypoxic conditions and metabolic substrate shortage typical of an ischemic insult, plates were centrifuged (233 x g, 5 minutes), the culture medium was replaced with glucose-free DMEM (#Cat: 11966025, Thermo Fisher Scientific), and the drugs

representing treatments for the experimental conditions were added to the medium (see Drugs and reagents for details). Plates were then placed into a Whitley H35 hypoxystation (Don Whitley Scientific, Yorkshire, UK) filled with humidified (65-70%) and hypoxic air (1% O₂, 5% CO₂, and 94% N₂) at 37°C. The chamber was sealed, and the OGD employed 6 h for both cell lines, producing "OGD plates". For the OGD/reoxygenation (OGD/R) condition, cells that were previously exposed to OGD had their medium changed after the 6 h of OGD to a complete medium containing glucose (4.5 g/L) and FBS (10 %) in the concentrations in which they were cultivated and were placed into the normoxic incubator for 24 h of reoxygenation in normoxic conditions. Cells kept in normoxia throughout all the period (6h + 24h)were used as controls with simultaneous medium changes as for OGD and OGD/R cells.

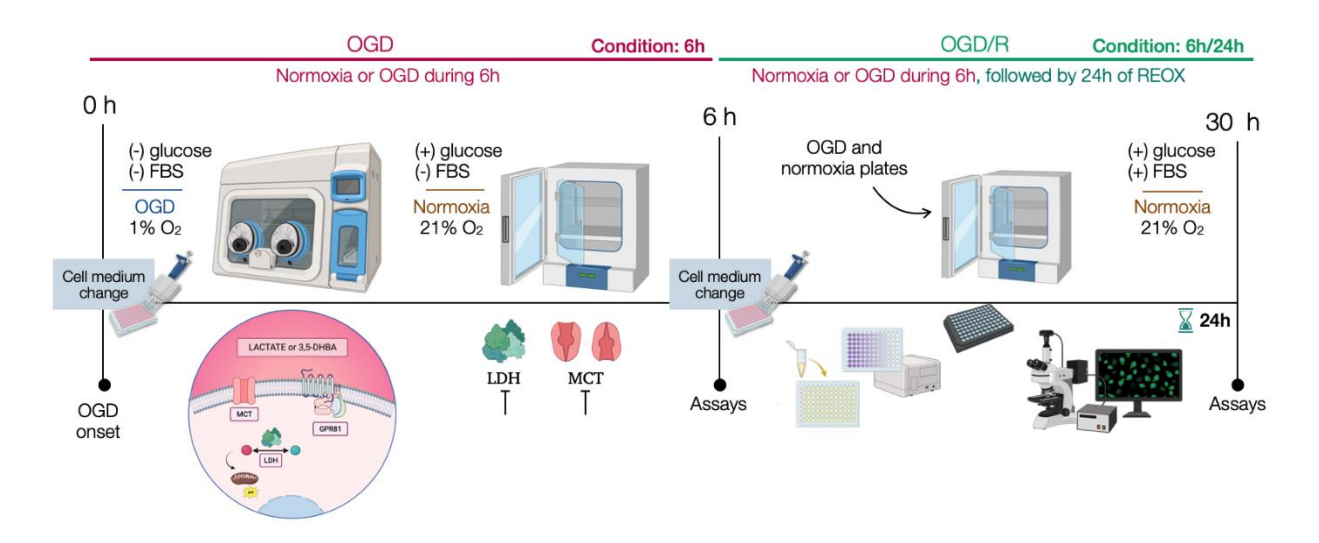


Figure 1. Schematic diagram of the oxygen-glucose deprivation (OGD) and OGD/reoxygenation (OGD/R) experimental procedures and respective conditions: cells were exposed to OGD for 6h; for OGD/R cells previously exposed to OGD were subjected to a subsequent 24h period of reoxygenation. Experiments were started by replace microglial and neuronal cell medium with glucose-free medium supplemented either with lactate or GPR81 agonist (3,5-DHBA). Both treatments were conducted alone or in combination with LDH or MCT inhibitors. OGD plates were placed into the hypoxic chamber (1% O₂) for 6 h; cells were immediately destined for assays in the end of these 6h. For the OGD/reoxygenation (OGD/R) condition, cells previously exposed to OGD had their medium changed after 6h of OGD to complete medium (glucose and FBS concentrations were restored; see 'Experimental conditions' for details) and were placed into the normoxic incubator for 24 h of reoxygenation in normoxic conditions (OGD/R condition). Normoxia groups were used as controls and had their medium changed simultaneously with OGD and OGD/R cells but kept in the cell culture incubator (21% O₂, 37°C).

Drugs and reagents

During the first 6 h of the experiment cells were exposed to OGD or their respective normoxic controls) were incubated with the following drugs dissolved in the cell culture medium: PBS (GibcoTM), equal volumes were used as vehicle control; L-lactate (71718, Sigma-Aldrich) 5 and 10 mM; GPR81 agonist, 3,5-Dihydroxybenzoic acid (3,5-DHBA, D110000, Sigma-Aldrich), 4 mM; LDH inhibitor, oxamate (ThermoFisher, A16532.06), 20 mM; MCT inhibitor, α-Cyano-4-hydroxycinnamic acid (4-CIN, C2020, Sigma-Aldrich), 1 mM. Lactate and 3,5-DHBA were dissolved in PBS, oxamate was dissolved in the respective DMEM (normal glucose and serum-free for normoxia

conditions and serum and glucose-free for OGD conditions), and 4-CIN was diluted in dimethyl sulfoxide (DMSO). Detailed information about the treatments is available in the Supplementary Table 1.

Experimental conditions

Four different experimental conditions were used in this study for both cell lines (BV-2 and SH-SY5Y): OGD, OGD/R, normoxia, and normoxia/"reoxygenation". OGD refers to oxygen and glucose deprivation for 6 h with no subsequent reoxygenation period. OGD/R refers to OGD for 6 h followed by 24 h of recovery in atmospheric oxygen conditions, as illustrated in Figure 1. Both normoxia and normoxia/"reoxygenation" are control conditions for OGD and OGD/R, respectively. Normoxia condition is characterized by normal oxygen levels for 6 h; normoxia/"reoxygenation" is characterized by normal oxygen levels for 6 h followed by a medium change and 24 h of "recovery" also under atmospheric oxygen conditions.. It is important to note that normoxic cells were treated with the same treatments as the OGD cells for all variables evaluated in the present study (except immunofluorescence and TNF-a release assays, where the control cells were PBS-treated only), ensuring that any observed effects are due to the treatments and not due to differences in experimental conditions. OGD cells in the hypoxic chamber were treated with serum-free and glucose-free medium and the normoxia control cells were treated with serum-free and normalglucose medium (DMEM GlutaMAXTM for BV-2 cells and DMEM/F12TM for SH-SY5Y cells) during the first 6 h of experiment. Cells that underwent the subsequent 24 h recovery period were removed from the hypoxic chamber (OGD) or from the incubator (normoxia) after 6 h, centrifuged (233 x g, 5 minutes), and had their medium changed to complete DMEM (10% FBS and 1% P/S). Then, cells were placed into the normoxic incubator at (37°C, 5% CO₂) for 24 h of recovery without any other treatment.

Cell viability assay

Following OGD or OGD/R, microglia and differentiated neuronal cells were incubated with $10 \,\mu\text{L}$ of 3-(4,5-dimethylthiazol-2-yl)-2,5-diphenyltetrazolium bromide (MTT) (M2128, Sigma-Aldrich) solution (5 mg/ml in PBS) per well, protected from light and placed into the cell incubator (5% CO₂, 37°C). After 2 h, the plates were centrifuged (233 x g, 5 minutes), the media supernatant was removed, and formazan crystals were dissolved using acidified isopropanol (0.02 N HCl in absolute isopropanol) [45]. The absorbance of the MTT reaction product was analyzed using a microplate reader at a wavelength of 570 nm, with background subtraction at 690 nm. Cell viability values were reported relative to the mean value of the control group (normoxia cells treated with PBS as the vehicle) from each independent experiment, which was repeated at least three times.

Extracellular lactate levels

After each experiment, the medium supernatant was collected and stored at -80°C until the day of the procedure. L-Lactate production was estimated by measuring lactate levels on culture supernatants with the enzymatic UV Lactate kit (K084-BioClin®) [46] according to the manufacturer. The reaction (L-lactate + NAD⁺ \leftrightarrow Pyruvate + NADH) was started by adding the reaction mix to the sample wells, incubated for 10 minutes, and the absorbance read in 340 nm in a microplate reader. The assay was performed in duplicate for each sample, and the absorbance was converted into mmol/L.

Intracellular pH measurements (pHi)

The intracellular pH of BV-2 cells was measured following OGD and OGD/R procedures using the BCECF-AM (14562, Sigma-Aldrich) dye. To allow appropriate cell attachment, on the day before OGD, BV-2 cells were seeded in a black 96-well plate (flat and transparent bottom) at a density of $4x10^4$ cells per well. Plates were centrifuged (233 x g, 5 minutes), and the medium was changed according to each experimental treatment (see Experimental conditions section). After OGD or OGD/R, cells were washed twice with HEPES-buffered saline (25 mM, pH 7.4) and then loaded with the pH-sensitive dye: $100 \mu L$ of BCECF-AM ($10 \mu M$) solution were added in each well, followed by a 30-minute incubation at 37° C in the dark to allow the BCECF-AM to diffuse into the cells and to become desterified to the fluorescent form, BCECF. The cells were washed twice with HEPES-buffered saline to remove any residual BCECF-AM, and the 96-well plates were read on a microplate reader (TECAN, Infinite® 200 PRO) equipped with excitation filters at 440 nm and 490 nm and an emission filter at 530 nm. After each experiment, a solution of a proton ionophore nigericin ($10 \mu M$) was added to a separate set of wells in the normoxia plate to induce the pHi to shift to known values of pH (6.0, 6.6, 7.0, 7.4, 8.0), enabling the generation of a standard curve for pH calibration. Ratios of BCECF fluorescence at Ex_{490}/Em_{530} and Ex_{440}/Em_{530} were acquired and converted to pHi from the standard curve generated with nigericin in each experiment [47, 48].

Immunofluorescence

Following OGD or OGD/R (and the respective normoxic control conditions) cells were harvested, centrifuged (233 x g, 5 minutes), fixed in 4% paraformaldehyde for 15 minutes at room temperature (RT), washed twice with PBS and stored at 4°C until staining. Cells were permeabilized using ammonium chloride (25 mM in PBS) for 5 minutes, followed by 10 minutes of 0.1% Triton-PBS. For the next steps, the coverslips were removed from the bottom of the 12-well plate and placed onto parafilm on a flat surface to start the blocking and cell staining procedure. Cells were incubated with 5% normal goat serum in PBS to block nonspecific binding for 30 minutes at RT. Immediately after blocking, cells were incubated for 2 h with primary antibodies: Rat X Tubulin (MAB1864, Sigma-Aldrich) (1:1000) for both cell lines, CD206 (Abcam, AB64693) (1:250) for BV-2 cells, Neurofilament light polypeptide (NEFL) (Cell Signalling, 2837) (1:500) for SH-SY5Y cells, followed by a 1 h incubation with the corresponding species-specific secondary antibody coupled with Alexa Fluor® staining: Goat Anti-Rabbit IgG H&L (Alexa Fluor® 488) (Abcam, ab150077); and Goat anti-Rat IgG H&L (Alexa Fluor® 647 nm) (Invitrogen, A-21247). The secondary antibody was incubated at RT. All secondary antibodies were diluted 1:500. Following secondary antibody incubations, the coverslips were washed three times with PBS and then carefully placed onto a glass slide containing 50 μL of Mounting Medium with DAPI (4′,6-diamidino-2-phenylindole) (ab104139, Abcam) for nuclei counterstain and final assembling.

Cell counting and neurite evaluation

Images from BV-2 and SH-SY5Y cells were captured using a ×40 oil immersion objective lens (Plan Apochromat 40x/1.4 Oil DIC M27) using a Zeiss LSM880 confocal microscope. Approximately six fields were

counted per condition, and the number of DAPI-positive (DAPI+) cells was expressed as a percentage of the control (normoxia) group from each respective replicate for both cell lines. The length of the longest neurite was determined on NEFL-stained cells (40x/1.4 Oil) using the ImageJ plugin, NeuronJ [49], and neurites were semi-automatically traced in order to determine the longest neurite length. Neurite evaluation was performed in approximately 110 ± 10 NEFL-positive cells per condition [49, 50].

TNF- α levels in the cell supernatant

TNF- α levels were measured in the BV-2 medium supernatant by enzyme-linked immunosorbent assay (ELISA) (TNF- α ELISA kit, Cat# 88-7324-86; Thermo Fisher Scientific) according to the manufacturer's protocol and expressed as μ IU/ml.

Statistics

The dataset was submitted to the Kolmogorov-Smirnov test to assess normality, and data were considered normal when p>0.05. Variables that fulfilled test requirements were analyzed through the two-way analysis of variance (ANOVA) (the effects of the factors are indicated in the figure legends), followed by Sidak's post-test for comparisons among multiple groups. Data are presented as mean ± standard deviation (SD) unless indicated otherwise. Data analysis of at least three independent experiments was performed using Graph Pad Prism 10.0.3 (GraphPad Software).

Results

Lactate rescues microglia viability following OGD challenge

After 6 h of OGD, there was a decrease in cell viability (p<0.0001, normoxia *versus* OGD), while the addition of 5 mM lactate attenuated this decline (p=0.0366, OGD + 5 mM lactate *versus* OGD + PBS) (Fig. 2a). Following a recovery span of 24 h, all treatments during the 6 h of OGD increased cell viability, except PBS (p=0.0015, *versus* OGD + PBS) (Fig. 2c). Extracellular lactate concentrations were higher in cultures that receive lactate administration in the medium, relative to PBS and 3,5-DHBA-treated cells after 6h of OGD or normoxia (p<0.0001) (Fig. 2c) Following 24 h of reoxygenation (after medium change and no additional treatment) all groups presented similar extracellular lactate concentrations (Fig. 2d), It suggests this lactate was produced and exported by microglia and is not residual lactate previously added to the culture.

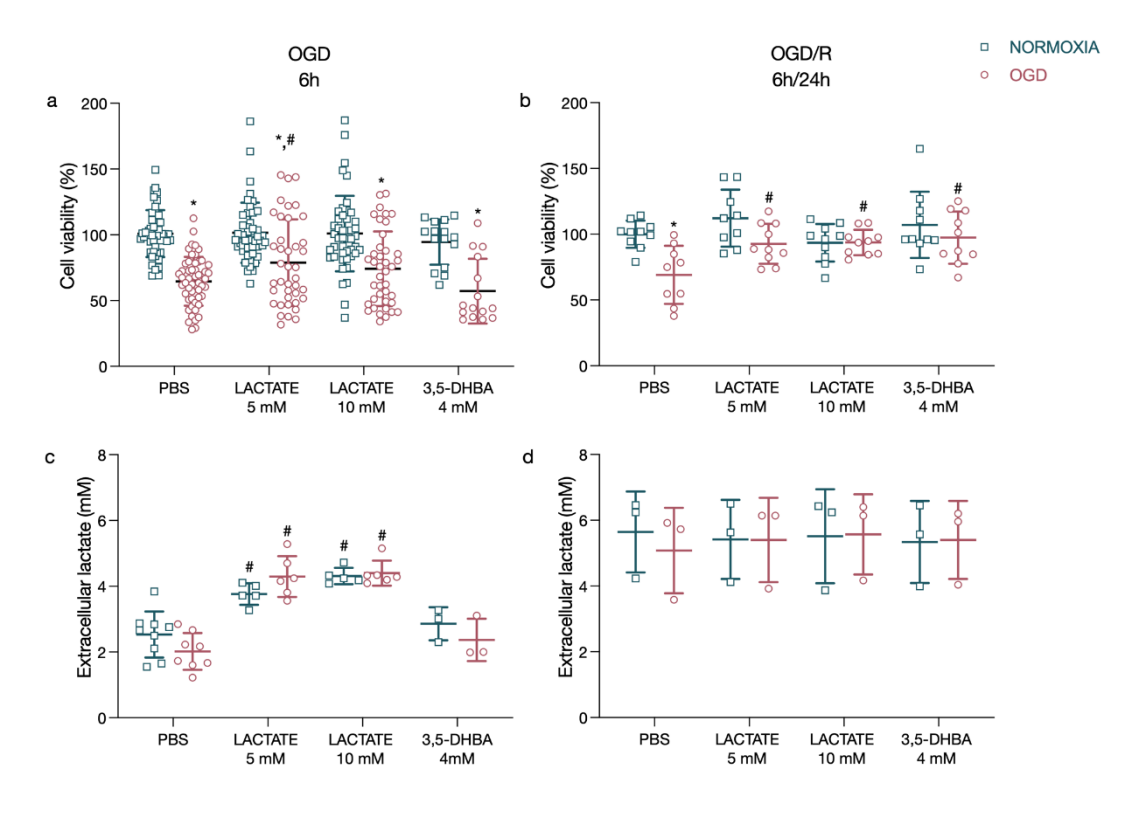


Figure 2. Effects of lactate and GPR81 activation on BV-2 viability (a and b) and extracellular lactate levels (c and d) after OGD or OGD/R. Cell viability was expressed as a percentage of the normoxia+PBS group in each experiment. Data were analyzed by two-way ANOVA, and the effects of factors "treatment" and "OGD" were tested. An effect of the factor "treatment" was observed in a $(F_{3,297} = 3.192, p<0.0001)$, b $(F_{3,70} = 4.293, p=0.0077)$, and c $(F_{3,37} = 44.05, p<0.0001)$, while an effect of the factor "OGD" was detected in a $(F_{1,297} = 93.98, p=0.024)$ and b $(F_{1,70} = 13.53, p=0.0005)$. No interaction was found between the factors. Sidak's post-hoc differences are indicated as *p<0.05 vs. respective normoxia group, # vs. PBS from the same condition (normoxia or OGD). Data were expressed as scatter plots with mean lines and standard deviation (SD) drawn for each experimental group. Squared or round dots represent individual values for each experimental replicate from at least three independent experiments.

Microglia survival relies on lactate metabolism

Inhibition of LDH by oxamate reduced cell viability, impairing lactate's rescue of cell viability following OGD (p<0.05, normoxia *versus* OGD, for all groups) (Fig. 3a). After reoxygenation, even normoxic cells had their viability reduced when they had been previously incubated with oxamate (p<0.05, normoxia + PBS *versus* normoxia + oxamate).Only 3,5-DHBA treatment increased cell viability (p<0.05, OGD + oxamate *versus* OGD + oxamate + 3,5-DHBA) (Fig. 3b). These results support the idea that the beneficial effects of lactate on cell viability seen during OGD require LDH activity and strengthens the role of lactate as a metabolic fuel. Inhibition of LDH also reduced lactate release after 6 h of incubation in normoxia and OGD conditions. Evidently, it was reverted when lactate, but not 3,5-DHBA, was added to the medium (Fig. 3c). A return of extracellular lactate levels to the values of the PBS group was seen for all the groups after 24 h recovery (Fig. 3d). Again, it is important to mention that the medium was changed at the end of the OGD and the beginning of the "reoxygenation" phase. This cleared oxamate from the medium and allowed recovery of LDH activity.

MCT-mediated lactate transport is required to maintain microglia viability

When MCT was blocked using the non-selective inhibitor 4-CIN, BV-2 cells exposed to OGD showed a reduction in viability relative to their respective normoxic controls, even when lactate was added to the medium (p<0.05, normoxia *versus* OGD, for all groups) (Fig. 3e). It suggests that transport inhibition prevents lactate on rescuing cell viability after OGD, as shown in Figure 2a. Moreover, the addition of 4-CIN to the medium reduced viability even in cells kept in normoxic conditions (p<0.05, normoxia + PBS *versus* normoxia + 4-CIN) (Fig. 3e). Following 24 h of reoxygenation, BV-2 cells which had previously been treated with lactate were able to recover viability (OGD + 5 mM lactate and OGD + 10 mM lactate *versus* OGD + PBS) (Fig. 3f). Extracellular lactate levels were increased after 6 h of OGD or normoxia in the presence of 4-CIN (p<0.05, *versus* PBS) (Fig. 3g). In contrast, after 24 h of recovery in a fresh medium, extracellular lactate levels were similar between 4-CIN-treated and PBS-treated cells, regardless of whether they were previously exposed to normoxia or OGD (Fig. 3h).

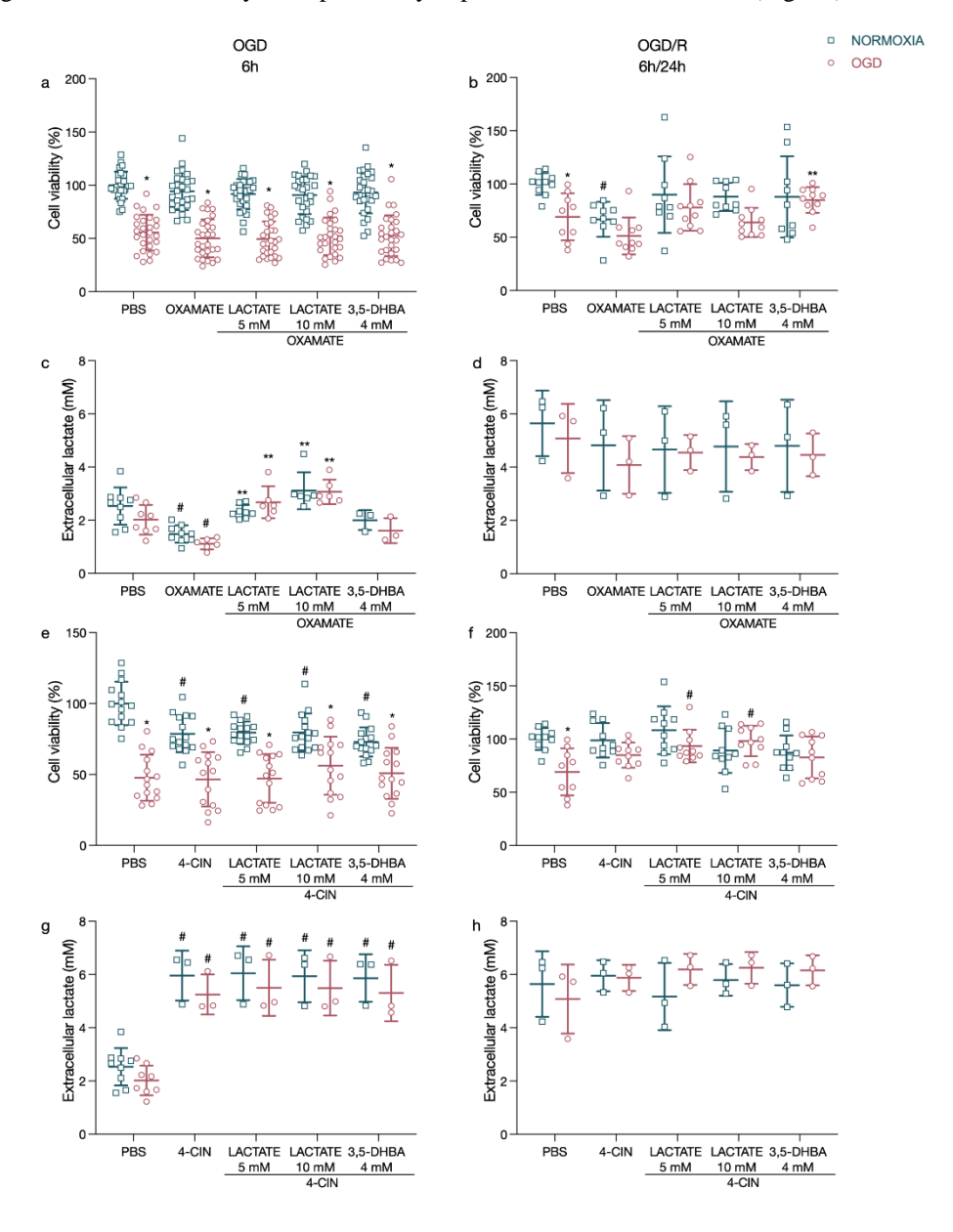


Figure 3. Effects of lactate and GPR81 activation on BV-2 viability (a, b, e, and f) and extracellular lactate levels (c, d, g, and h) after OGD and OGD/R in the presence of either a LDH inhibitor, oxamate (a, b, c, and d) or a MCT inhibitor, 4-CIN (e, f, g, and h). Cell viability was expressed as a percentage of the normoxia+PBS group in each experiment. Data were analyzed by two-way ANOVA, and the effects of factors "treatment" and "OGD" were tested. An effect of the factor "treatment" was observed in b ($F_{4,85} = 5.115$, p=0.0010), c ($F_{4,54} = 23.26$, p<0.0001), e ($F_{4,134} = 3.027$, p<0.019), f ($F_{4,89} = 2.985$, p=0.0231), and g ($F_{4,31} = 41.97$, p<0.0001), while an effect of "OGD" was detected in a ($F_{1,260} = 407.7$, p<0.0001), b ($F_{1,85} = 14.58$, p=0.0003), e ($F_{1,134} = 159.4$, p<0.0001), and f ($F_{1,89} = 9.986$, p=0.0022). Interaction between factors was found in e ($F_{4,134} = 4.326$, p=0.0025) and f ($F_{4,89} = 3.491$, p=0.0107). Sidak's post-hoc differences are indicated as *p<0.05 vs. respective normoxia group, ** vs. oxamate from the same condition (normoxia or OGD), and # vs. PBS from the same condition (normoxia or OGD). Data were expressed as scatter plots with mean lines and standard deviation (SD) drawn for each experimental group. Squared or round dots represent individual values for each experimental replicate from at least three independent experiments.

BV-2 intracellular pH changes after lactate metabolic modulation during OGD

To check for intracellular acidification, pH measurements were performed in BV-2 cells after OGD and after OGD/R. Indeed, 6 h of OGD reduces pHi (Fig. 4a, p<0.05, normoxia *versus* OGD, for PBS and 5mM lactate groups). However, pHi returned to baseline values after 24 h of reoxygenation in previously treated with lactate (Fig. 4b). When LDH was inhibited, pHi was reduced after OGD regardless of the treatment (p<0.05, normoxia *versus* OGD, for all groups) (Fig 4c). However, during reoxygenation cells returned their pHi to normoxia values, except for 3,5-DHBA group (p<0.05, normoxia + oxamate + 3,5-DHBA *versus* OGD + oxamate + 3,5-DHBA) (Fig. 4d). MCT blocking did not alter the pHi itself but led to increased acidification in lactate or 3,5-DHBA-treated groups (p<0.05, normoxia *versus* OGD, for 5mM lactate and 3,5-DHBA) (Fig. 4e). The effects of 4-CIN on pHi levels seem to be attributed to its presence in the cell supernatant, without causing subsequent cell changes, as it was innocuous during reoxygenation – when cells when cells were exposed to a fresh medium (Fig. 4f).

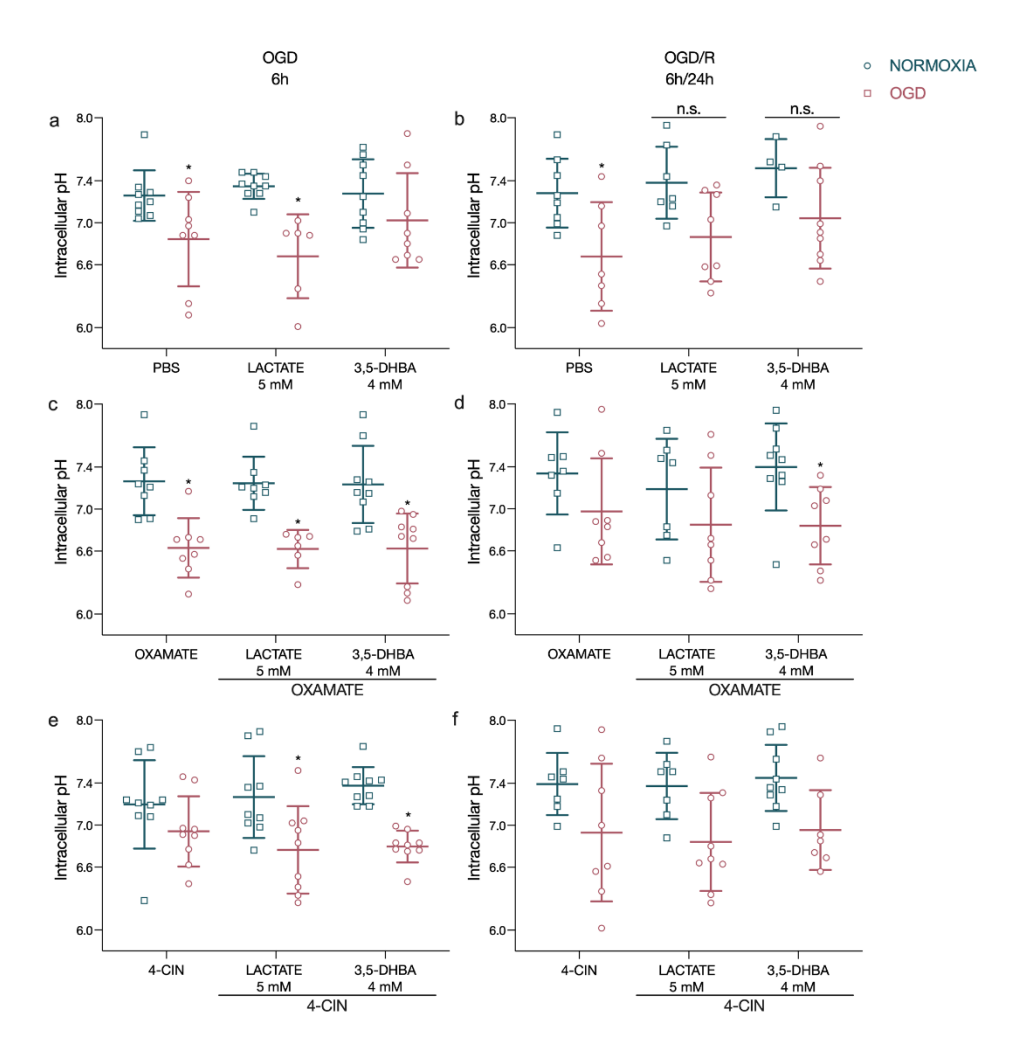


Figure 4. Effects of lactate and GPR81 activation on BV-2 intracellular pH after OGD or OGD/R in the absence (a and b) or in the presence of either a LDH inhibitor, oxamate (c and d), or a MCT inhibitor, 4-CIN (e and f).. Data were analyzed by two-way ANOVA, and the effects of factors "treatment" and "OGD" were tested. An effect of the factor "OGD" was detected in a $(F_{1,43} = 20.26, p < 0.0001)$, b $(F_{1,37} = 16.46, p = 0.0002)$, c $(F_{1,42} = 49.72, p < 0.0001)$, d $(F_{1,41} = 9.935, p = 0.0030)$, and e $(F_{1,41} = 15.60, p = 0.0003)$. No effect of the factor "treatment," or interaction between the factors was found. Sidak's post-hoc differences are indicated as *p<0.05 vs. respective normoxia group. Data were expressed as scatter plots with mean lines and standard deviation (SD) drawn for each experimental group. Squared or round dots represent individual values for each experimental replicate from at least three independent experiments.

Reoxygenation influences the number of BV-2 cells

To visualize the overall distribution of microglia, DAPI+ nuclei labeled cells were counted after OGD and after OGD/R (Fig. 5a). Two-way ANOVA indicated an effect of the treatment (p<0.05). Additionally, it was found that the number of DAPI+ nuclei of microglial cells decreased after OGD (Fig. 5b) and OGD/R compared to normoxic conditions (p<0.05). However, after reoxygenation an increase in the overall number of cells was seen in cultures previously treated either with lactate or 3,5-DHBA (p<0.05, *versus* OGD/R) (Fig. 5c).

Lactate mitigates BV-2 pro-inflammatory response following reoxygenation

Following OGD/R (6 h of OGD and 24 h of reoxygenation), a remarkable increase in the levels of TNF-a(p<0.05) was observed relative to OGD (6h of OGD with no recovery). However, this late inflammatory response was prevented by the previous addition of lactate or GPR81 agonist to the culture medium (Fig. 5e). These findings suggest that lactate treatment during OGD can directly reduce the later inflammatory response of BV-2 cells seen during reoxygenation.

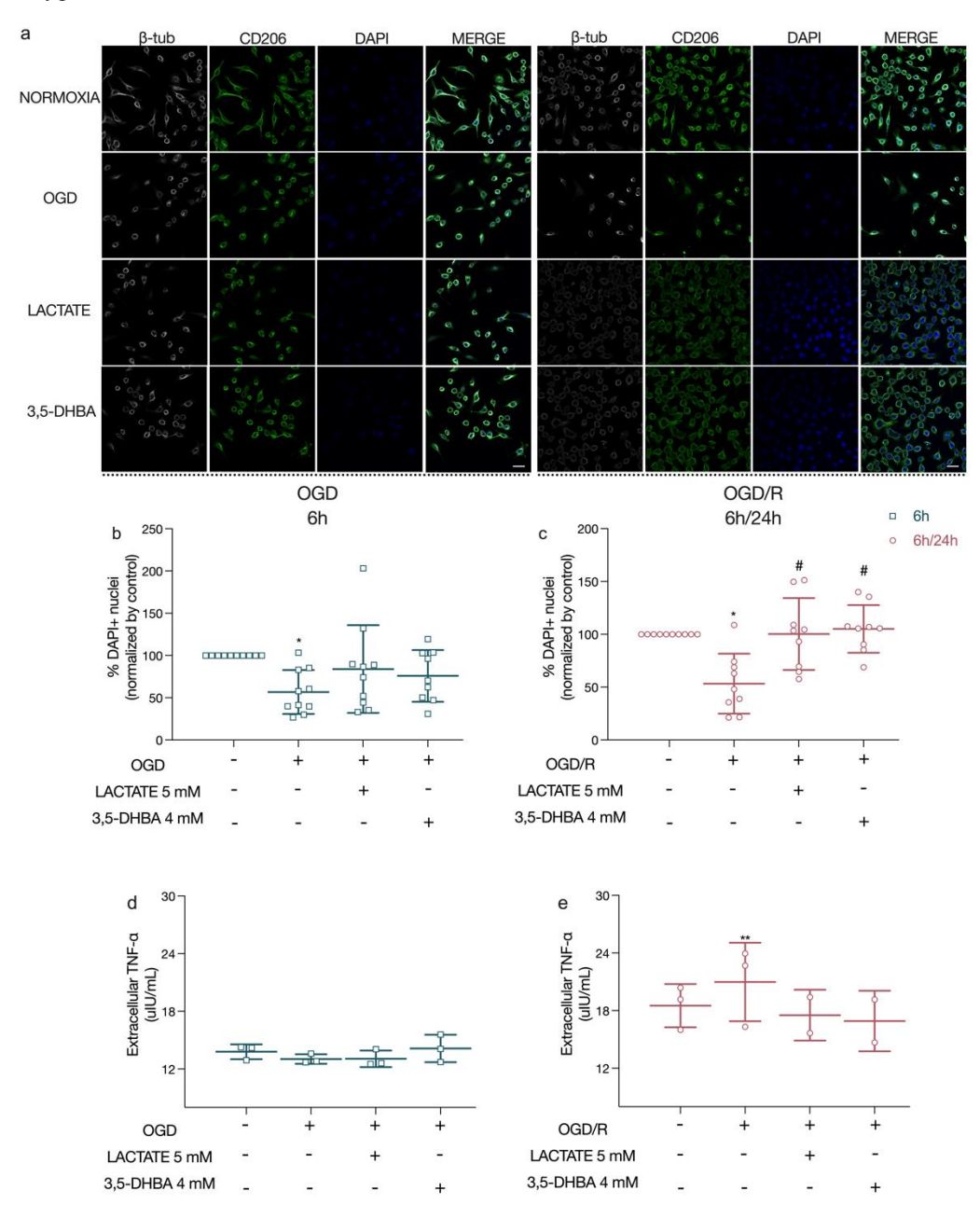


Figure 5. Effects of lactate and GPR81 activation on the number of BV-2 cells and the level of TNF- α . BV-2 representative immunostaining images are shown in a. Cells had their cytoskeleton labeled with anti- β -tubulin (white

stain) and anti-CD206 (green stain) and were counterstained with DAPI (blue stain). DAPI+ nuclei were counted after OGD ("OGD 6h", b) and OGD/R ("OGD/R 6h/24h", c). Microglial TNF- α release was quantified in cell supernatant also after OGD (d) and OGD/R (e). Data were analyzed by two-way ANOVA, and the effects of factors "treatment" and "recovery" were tested. Data from b and c were statistically analyzed together, as well as data from d and e (results were split into two separate charts for better visualization). An effect of the factor "treatment" was observed for "b and c" (F(3,68) = 9.050, p<0.0001), and an effect of the factor "recovery" was observed for "d and e" (F(1,14)=27.33, p=0.0001). No interaction between the two factors was found. Sidak's post-hoc differences are indicated as *p<0.05 versus normoxia, **p<0.05 versus OGD, #p<0.05 versus OGD/R. Data were expressed as scatter plots with mean lines and standard deviation (SD) drawn for each experimental group. Squared or round dots represent individual values for each experimental replicate from at least three independent experiments. Scale bar: 20 μ m.

Lactate and GPR81 activation rescue neuronal viability following OGD challenge

The viability of differentiated SH-SY5Y cells decreased after OGD (p<0.05, normoxia + PBS *versus* OGD + PBS). Although 10 mM lactate did not rescue cell viability (p<0.05, normoxia + 10 mM lactate *versus* OGD + 10 mM lactate), 5 mM lactate and 3,5-DHBA treatments abrogated this decline (Fig. 6a). After OGD/R, all groups exhibited reduced cell viability (p<0.05, normoxia *versus* OGD, for PBS, 10 mM lactate and 3,5-DHBA groups) except the lactate 5 mM group (Fig. 6b). Following OGD, extracellular lactate concentrations were constant for all treatments in the normoxic conditions. In contrast, they were increased in the cell supernatant of OGD-exposed SH-SY5Y cells treated with lactate (10 mM) when compared to PBS or 3,5-DHBA (p<0.05, *versus* OGD + 10 mM lactate) (Fig. 6c). Following reoxygenation, the extracellular lactate concentrations were similar, regardless of the OGD or treatment (Fig. 6d).

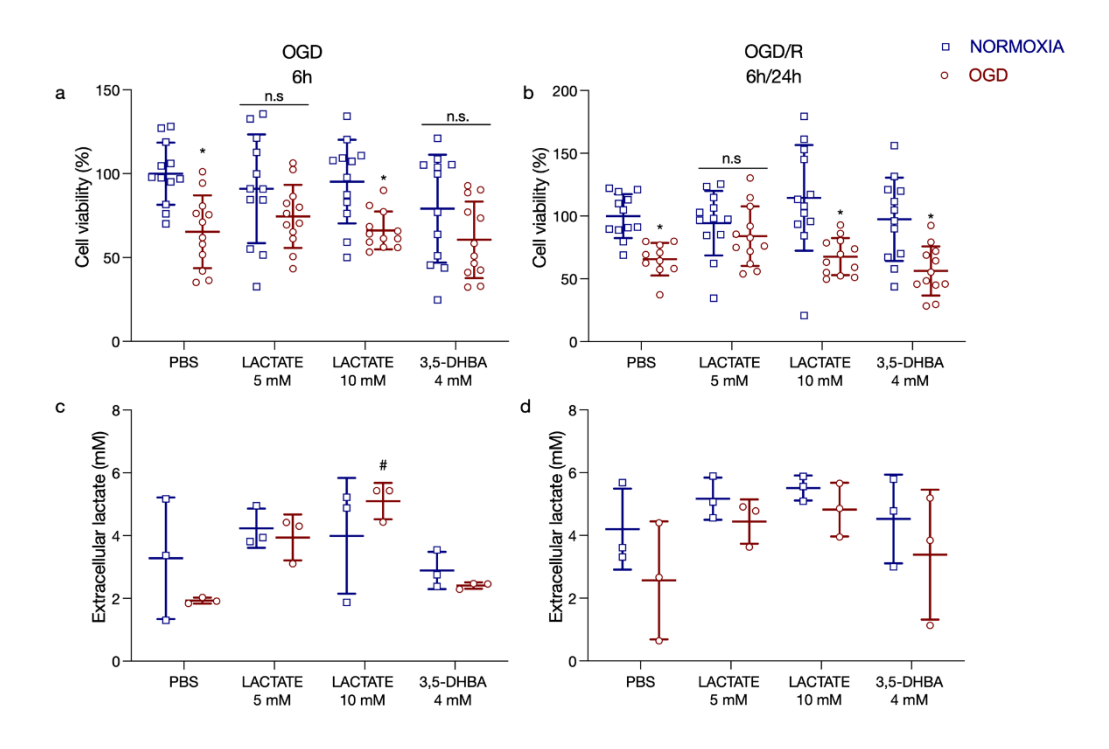


Figure 6. Effects of lactate and GPR81 activation on differentiated SH-SY5Y cells viability (a and b) and extracellular lactate levels (c and d) after OGD and OGD/R. Cell viability was expressed as a percentage of the normoxia+PBS group in each experiment. Data were analyzed by two-way ANOVA, and the effects of factors "treatment" and "OGD" were tested. An effect of the factor "treatment" was observed in c (F_{3,16}=5.394, p=0.0093), while an effect of "OGD"

was detected in a $(F_{1,88}=25.92, p<0.0001)$ and b $(F_{1,86}=39.17, p<0.0001)$. No interaction was detected between the factors. Sidak's post-hoc differences are indicated as *p<0.05 vs. respective normoxia group, and #p<0.05 vs. PBS from the same condition (normoxia or OGD), "n.s" means not significant. Data were expressed as scatter plots with mean lines and standard deviation (SD) drawn for each experimental group. Squared or round dots represent individual values for each experimental replicate from at least three independent experiments.

Neuronal viability relies on lactate metabolism even in normoxia

When exposed to oxamate, SH-SY5Y cells exhibited a remarkable decrease in cell viability even under normoxia (p<0.05, *versus* normoxia + PBS), except for those also treated with 3,5-DHBA. No differences were observed in oxamate-treated cells after OGD compared to their respective normoxia controls (Fig. 7a). Interestingly, after OGD/R, normoxic cells previously treated with oxamate recovered their viability. Recovery of neuronal viability after oxamate was removed from the medium occurred exclusively in cells maintained in normoxic conditions, as OGD-treated groups remained with lower viability following 24 h of reoxygenation (p<0.05, normoxia *versus* OGD, for all treatments) (Fig. 7c). Lactate extracellular levels were reduced in the medium of SH-SY5Y cells when exposed to oxamate alone after OGD (p<0.05, PBS *versus* oxamate) (Fig 7b). Following 24 h of reoxygenation, two-way ANOVA detected an overall effect of OGD on decreased extracellular lactate levels (p<0.05, normoxia *versus* OGD) (Fig. 7d).

Lactate transport influences neuronal viability and extracellular lactate levels

Inhibition of MCTs decreased SH-SY5Y cell viability after OGD (p<0.05, normoxia *versus* OGD), except when cells were incubated with 10 mM lactate or 3,5-DHBA groups (Fig. 7e). After OGD/R, MCT-blocked cells from OGD groups presented the same cell viability values as normoxia cells, regardless of the treatments (Fig. 7f). Considering extracellular lactate, all MCT-inhibited cells displayed increased lactate levels (p<0.05, 4-CIN *versus* PBS), with 10 mM lactate group showing the higher values (p<0.05, 4-CIN and 3,5-DHBA *versus* 10 mM lactate) after 6 h of OGD (Fig. 7g). Neurons incubated with 4-CIN and treated with 10 mM lactate sustained their high lactate levels even after 24 h of recovery (p<0.05, OGD + PBS *versus* OGD + 10 mM lactate) (Fig. 7h).

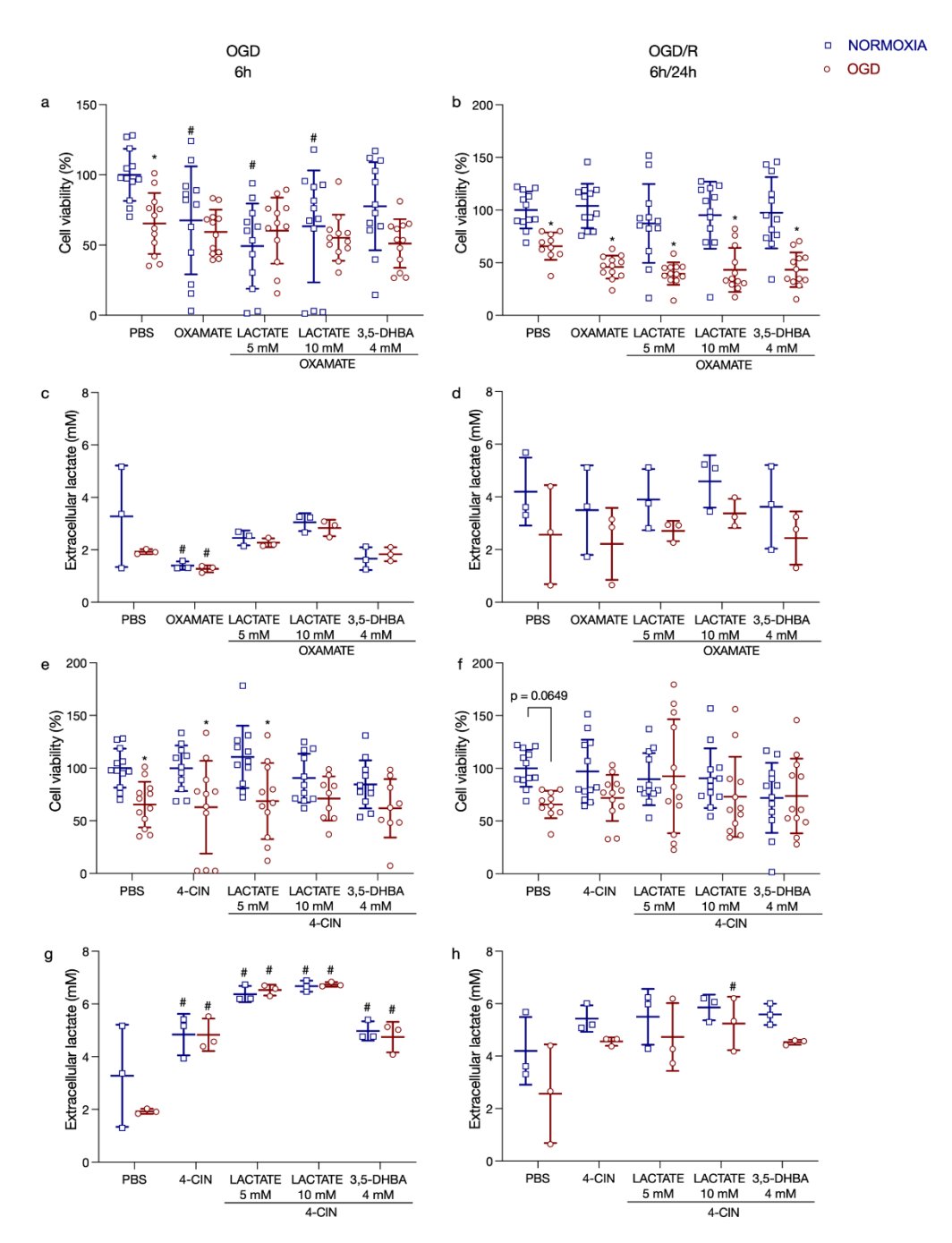


Figure 7. Effects of lactate and GPR81 activation on SH-SY5Y viability (a, b, e, and f) and extracellular lactate levels (c, d, g, and h) after OGD and OGD/R in the presence of either a LDH inhibitor, oxamate (a, b, c, and d) or a MCT inhibitor, 4-CIN (e, f, g, and h),. Cell viability was expressed as a percentage of the normoxia+PBS group in each experiment. Data were analyzed by two-way ANOVA, and the effects of factors "treatment" and "OGD" were tested. An effect of the factor "treatment" was observed in a $(F_{4,110} = 3.8, p=0.0062)$, c $(F_{4,20} = 5.796, p=0.0029)$, g $(F_{4,20} = 29.84, p<0.0001)$, and h $(F_{4,20} = 4.269, p=0.0117)$, while an effect of "OGD" was detected in a $(F_{1,110} = 7.432, p=0.0075)$, b $(F_{1,108} = 129.9, p<0.0001)$, d $(F_{1,20} = 7.786, p=0.0113)$, e $(F_{1,122} = 35.94, p<0.0001)$, f $(F_{1,98} = 33.87, p<0.0001)$, and h $(F_{1,20} = 7.556, p=0.0124)$. Interaction between factors was found in a $(F_{4,110} = 2.679, p=0.0354)$. Sidak's post-hoc differences are indicated as *p<0.05 vs. respective normoxia group, and # vs. PBS from the same condition (normoxia or OGD). Data were expressed as scatter plots with mean lines and standard deviation (SD) drawn for each experimental group. Squared or round dots represent individual values for each experimental replicate from at least three independent experiments.

Reoxygenation impairs neurite elongation following OGD

SH-SY5Y DAPI+ nuclei counting was also performed in cells counterstained with NEFL and β -tubulin (Fig. 8a) immediately after OGD (Fig. 8b) and following OGD/R (Fig. 8c). Two-way ANOVA did not show any effect of the factors "treatment" or "reoxygenation" in total nuclei quantification and neurite elongation parameters. The longest neurite length did not change during the OGD period (Fig. 8d), whereas after OGD/R (Fig. 8e), the OGD-exposed neurons depicted shorter lengths compared to the lactate-treated ones (p<0.05, OGD *versus* OGD+lactate 5 mM).

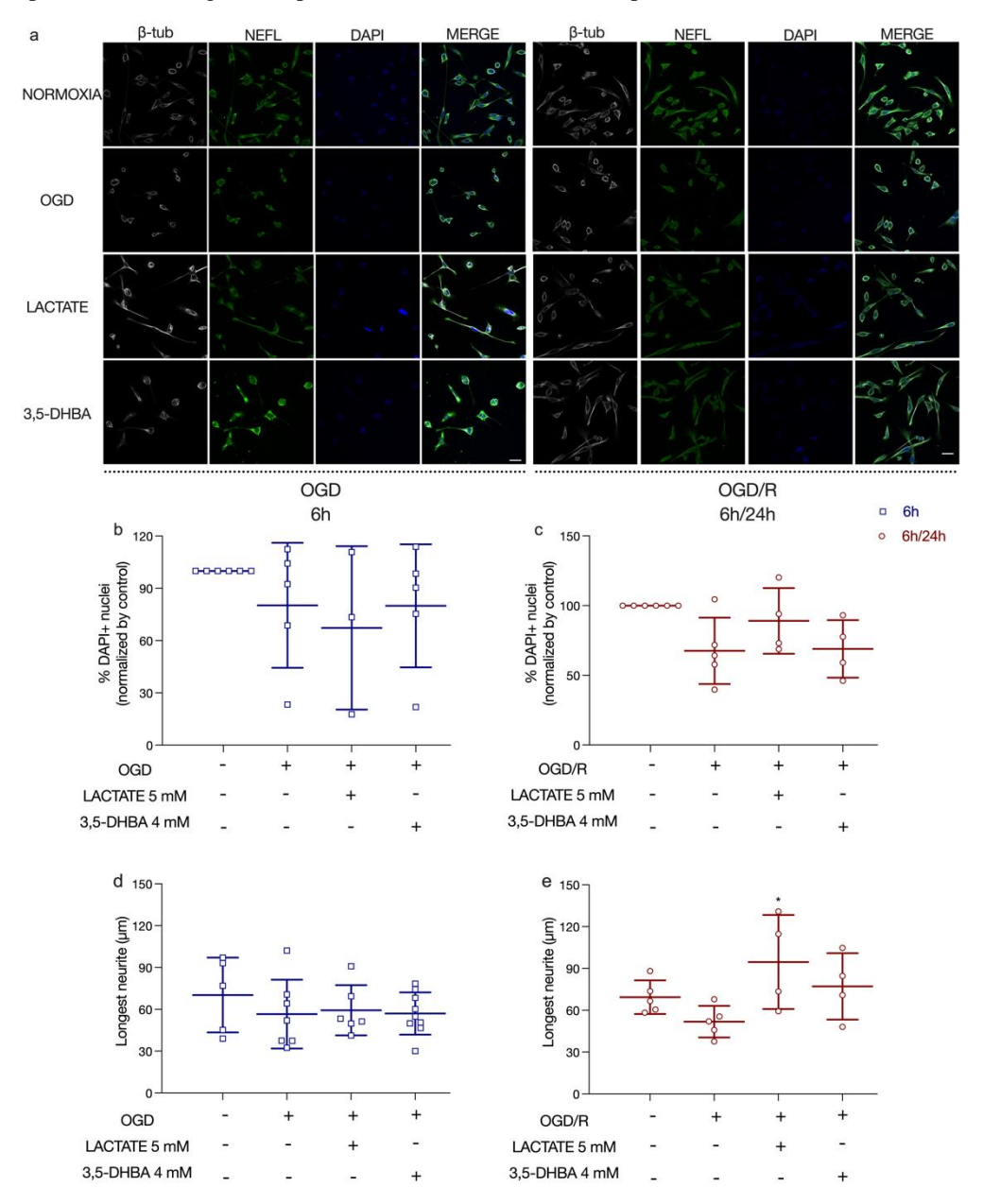


Figure 8. Effects of lactate and GPR81 activation on the number of SH-SY5Y cells and neurite elongation. SH-SY5Y representative immunostaining images are shown in a. (white: anti-β-tubulin; green: anti-NEFL; blue: DAPI). DAPI+ nuclei and neurite assessment were evaluated after OGD ("OGD 6h", b and d) and OGD/R ("OGD/R 6h/24h", c and e).. Data were analyzed by two-way ANOVA, and the effects of factors "recovery" and "condition" were tested. No effect of factors or interaction was detected by two-way ANOVA. Sidak's post-hoc differences are indicated as

*p<0.05 vs OGD/R. Data were expressed as scatter plots with mean lines and standard deviation (SD) drawn for each experimental group. Squared or round dots represent individual values for each experimental replicate from at least three independent experiments. Scale bar: 20 μm.

Discussion

From cellular waste to metabolic fuel, nowadays also postulated as a signaling molecule, lactate roles are being constantly unraveled in recent compelling studies [3, 4, 38, 40, 51]. The metabolic actions of lactate depend highly on lactate transporters and LDH isoenzymes, whereas the signaling properties are associated with the activation of the HCAR1/GPR81 receptor. Both of these mechanisms by which lactate operates are independent of each other. Thus, differentiating lactate roles in the CNS and the mechanisms by which lactate orchestrates such responses might provide the groundwork for the clinical use of lactate in pathological conditions.

Here, we provide evidence that lactate metabolism plays a significant role in cell survival during OGD/R. The protocol employed in the present study used two different timepoints: an acute (OGD for 6h) and a late (OGD/R: OGD for 6h followed by a 24 h period of reoxygenation). Lactate, lactate receptor agonist and inhibitors of lactate metabolism and transport were always added to the medium during OGD, and the medium was changed before reoxygenation was started. To the best of our knowledge, this is the first study to use lactate as a treatment for BV-2 and SH-SY5Y cell lines exposed to a hypoxic and glucose-free environment in order to understand how the exogenous lactate supplied during OGD reduces microglial and neuronal death. Our data indicate that lactate availability *during* OGD increases cell viability and promotes long-term protective effects observed later, after reoxygenation, in both, microglial and neuronal cell lines. It has already been argued that lactate accumulation during hypoxia *in vitro* allows the recovery of synaptic function upon reoxygenation [52]. Interestingly, a recent study showed that lactate treatment during reoxygenation also increased BV-2 cells viability, which decreased neuronal apoptosis when co-cultured with primary cultured neurons [28].

Immediately after OGD, lactate-treated BV-2 cells maintained higher concentrations of lactate in the cell medium (approximately 4 mM, similar to physiological concentrations found in the CNS). Lactate PBS and 3,5-DHBA-treated cells depicted 2-fold lower concentrations during hypoxia as compared to reoxygenation. A reduction in lactate release was observed in Müller cells when incubated with the GPR81 agonist in the presence of glucose but not in its absence [38]. Here, it is important to mention that even though we refer to our insult as OGD, the glucose-free medium does not guarantee the total absence of glucose to the medium since there can be the synthesis and release of glucose from substrates such as amino acids present in the medium (although we believe that concentrations would be very low in this situation). On the other hand, it has been shown that not only the complete absence but even low concentrations of glucose (0-5 mM) are detrimental to neurons [53]. Notwithstanding, the lack of glucose measurements in the cell medium is a limitation of our study.

To address the contribution of lactate metabolism for cell viability, we used oxamate to inhibit LDH in BV-2 and differentiated SH-SY5Y cell lines during OGD. LDH inhibition reduced cell survival and the extracellular levels of lactate in either normoxia or OGD-exposed cells, possibly due to the LDH committals in NAD⁺ recycling, which may have undermined the redox state and the lactate/pyruvate ratio. Indeed, lactate-mediated neuroprotection seems conditional to microglial and neuronal lactate oxidation, as LDH inhibition abolished such effects. This reinforces

exogenous lactate can be a prompt fuel used for injured cells. In line with our results, lactate could not exert its neuroprotective when oxamate was used to inhibit LDH in vivo following neonatal hypoxia-ischemia [4]. Even though it indicates that lactate is effective after the insult (i.e., during the phase of reperfusion/reoxygenation), here we also observed a protective effect of the lactate administered during OGD. Interestingly, while SH-SY5Y viability was reduced during normoxia upon LDH inhibition, it was rescued when oxamate was removed from the medium, suggesting that lactate metabolism is essential for neuronal survival, even in physiological (i.e., normoxic) conditions [53]. MCT-driven transport is required for lactate uptake and oxidation. In this sense, it is worth mentioning that MCT4 loss impairs microglial synaptic pruning [54]; otherwise, MCT1 participates in microglial classical activation through glycolysis [17] and seems to play a beneficial role in ischemia [16]. Herein, MCT inhibition sustained extracellular lactate levels and reduced BV-2 viability even during normoxia, possibly due to a disruption in lactate uptake and metabolization. One could argue that these effects on cell viability are attributed to metabolic impairment, as 4-CIN has been reported to be a metabolic inhibitor for neurons and astrocytes by reducing oxidative metabolism [55]. Interestingly, when 4-CIN was removed from the cell medium over 24 h of recovery, BV-2 and SH-SY5Y, previously exposed to OGD, recovered viability. It strengthens that the role of lactate in improving cell survival requires its uptake (and possible metabolization). An alternative flow of lactate across cell membranes could also explain the increased extracellular lactate concentration in 4-CIN treated groups: 1) there might be a pharmacological competition between 4-CIN and lactate for the MCT; 2) connexins also allow lactate flow across cell membrane [56]. Therefore, lactate may still be released into the extracellular space when MCT is in 56hibited Sotelo-Hitschfeld and colleagues showed that other channels could also promote lactate movement across cellular compartments [57]. Thus, unraveling the mechanisms involved in lactate flow across neural cells is mandatory. Since the pattern of MCT isoforms distribution differs over time [21], one could stress that neural plasticity during development is the explanation for brain fluctuation in the preference for energy sources to sustain metabolic needs - even for higher brain functions. In that regard, lactate provides the energy required for neuronal protein synthesis involved in long-term memory processes in adult rats [58], while the regulation of the GPR81/cAMP/PKA pathway by aerobic exercise promotes synaptic growth and improves cognitive function in Alzheimer's [59].

Conversely, lactate accumulation has been linked to cytotoxic effects (i.e., cell acidification and disruption of the redox status) [60, 61]. However, our data show that pHi changes are unrelated to lactate but to OGD, in line with previous reports [62, 63]. Normoxia BV-2 cells maintain physiological pHi despite lactate loads of 5 and 10 mM, while OGD cells exhibited a reduction in pHi. Even after 24 h of reoxygenation, OGD influence was remarkable and sustained. Similarly, a previous study demonstrated that pH changes affect cell proliferation in an embryonic stem cell line, in which lactate was suggested to provide the fuel (dependent on LDH and MCT) to surviving cells that could adapt to the environment [64]. Limitations to describe these mechanisms in OGD-exposed microglia include the lack of extracellular pH measurements and intracellular lactate concentrations to compare with intracellular and extracellular values, respectively.

Notwithstanding changes in intracellular pH are clear, the release of TNF- α by BV-2 cells also shed light on the mechanisms related to lactate and GPR81 activation during OGD/R. Lactate administered during OGD prevented the increase in TNF- α levels seen in BV-2 cells during reoxygenation, suggesting an action of lactate on the long-term

inflammatory response. BV-2 cell viability, reduced during OGD, was rescued during reoxygenation if lactate or 3,5-DHBA were available previously during OGD, demonstrating that besides fueling microglia, lactate promotes long-term benefits. Such mechanism seems to be determined by the reoxygenation, in line with two previous microglial protocols that evaluated cells exposed to 2 h [65] or 3 h [66] of OGD, followed by 12 h of reoxygenation. Peripheral anti-inflammatory effects of lactate (i.e., reduced NF-κB and inflammasome activation) have been attributed to GPR81 signaling [33], whereas lactate inhibited NF-κB pathway and triggered a protective response via HIF-1α activation following OGD in microglia [28]. The reduction in the number of microglial cells and the increase in TNF-α release is usually associated with the delayed responses typically observed during the reperfusion period [65, 67]. These findings suggest that the addition of lactate to the medium and GPR81 activation during OGD could trigger reparative mechanisms that produce long-term protective effects.

Besides microglial, neuronal responses to OGD were assessed in terms of projection lengths and metabolic modulation. The neuroblastoma-derived cell line used here is a widely used model to study neuronal development [68, 69]. This lineage is usually exposed to a differentiation protocol [70] to produce a population of cells with morphological and functional features similar to mature neurons [71]. The neuronal-like features include morphological elongation of neurites (processes that arose from soma longer than the cell body [72]), which can be assessed using neurofilament markers (critical proteins that sustain axonal structure and neurite outgrowth)[73, 74]. Here, we have shown that lactate-treated neurons displayed a remarkable increase in neurite length after reoxygenation, suggesting lactate influences key morphological patterns of differentiated neurons [75]. It has been shown that primary cell cultures of microglia reversibly displayed elongation of cell processes upon lactate treatment in a time-dependent effect [76]. Even though it was described in microglial cells, it is possible the occurrence of a similar mechanism activated by lactate in neurons, as observed herea While microglia may assume a phagocytic phenotype, they may shift their metabolic preferences, increasing glycolytic rate and lactate production [77]. Lactate fits into that perspective as it mediates muscle regeneration by shifting macrophages to a state that allows revascularization and regeneration after ischemia [78], modulates microglial inflammatory responses after OGD [28], influences microglial phagocytic capacity [42] and, as outlined here, is engaged in neuronal and microglial survival in face of OGD. However, our findings should be interpreted with caution, taking into account the effects of the abrupt glucose withdrawal concomitant with lactate addition or GPR81 activation during OGD. It is a limitation of the present study the lack of an approach evaluating this exchange of metabolic substrates. Nevertheless, it is important to note that the protective properties shown here are primarily associated with lactate rather than pyruvate, as pyruvate was not able to recover cell viability during OGD (Supplementary Figures 1 and 2).

Whether the therapeutic effects of lactate during OGD are reproduced in primary cell cultures (or co-cultures to evaluate intercellular responses) remains to be investigated. The absence of a deeper investigation of the role of lactate in microglia-neuron crosstalk certainly includes a weak point of our work, as well as the lack of experiments showing the pattern of expression of GPR81 during OGD and OGD/R. In this sense, as there are studies showing the existence of GPR81 in neurons [79–81] but less evidence available to support its presence in microglia, we run a supplementary experiment to confirm the expression of GPR81 in BV-2 cells in basal conditions using immunohistochemistry (Suplemmentary Figure 3). Nevertheless, further studies are needed to build a more complete

picture of the mechanisms triggered by lactate and GPR81 activation – which is necessary to consider the therapeutic use of lactate. Overall, our data show that the metabolic contribution of lactate is crucial for circumventing the harmful implications of OGD, probably by enfolding the energy failure in suffering cells. Unraveling the cell-specific mechanisms of action of lactate will provide valuable insights into the complex interplay between metabolism and cell signaling and how these processes are regulated under pathophysiological conditions.

References

- 1. Berthet C, Lei H, Thevenet J, et al (2009) Neuroprotective role of lactate after cerebral ischemia. J Cereb Blood Flow Metab 29:1780–1789. https://doi.org/10.1038/jcbfm.2009.97
- 2. Hamdy N, Eide S, Sun H-S, Feng Z-P (2020) Animal models for neonatal brain injury induced by hypoxic ischemic conditions in rodents. Exp Neurol 334:113457. https://doi.org/10.1016/j.expneurol.2020.113457
- 3. Tassinari IDÁ, Andrade MKG, da Rosa LA, et al (2020) Lactate Administration Reduces Brain Injury and Ameliorates Behavioral Outcomes Following Neonatal Hypoxia–Ischemia. Neuroscience 448:191–205. https://doi.org/10.1016/j.neuroscience.2020.09.006
- 4. Roumes H, Dumont U, Sanchez S, et al (2021) Neuroprotective role of lactate in rat neonatal hypoxia-ischemia. J Cereb Blood Flow Metab 41:342–358. https://doi.org/10.1177/0271678X20908355
- Azevedo PN, Zanirati G, Venturin GT, et al (2020) Long-term changes in metabolic brain network drive memory impairments in rats following neonatal hypoxia-ischemia. Neurobiol Learn Mem 171:107207. https://doi.org/10.1016/j.nlm.2020.107207
- 6. Buscemi L, Blochet C, Magistretti PJ, Hirt L (2021) Hydroxycarboxylic Acid Receptor 1 and Neuroprotection in a Mouse Model of Cerebral Ischemia-Reperfusion. Front Physiol 12:689239. https://doi.org/10.3389/fphys.2021.689239
- 7. You Q, Lan X-B, Liu N, et al (2023) Neuroprotective strategies for neonatal hypoxic-ischemic brain damage: Current status and challenges. Eur J Pharmacol 957:176003. https://doi.org/10.1016/j.ejphar.2023.176003
- 8. Molloy EJ, Branagan A, Hurley T, et al (2023) Neonatal encephalopathy and hypoxic-ischemic encephalopathy: moving from controversy to consensus definitions and subclassification. Pediatr Res. https://doi.org/10.1038/s41390-023-02775-z
- 9. Deng Q, Wu C, Liu TC-Y, et al (2023) Exogenous lactate administration: A potential novel therapeutic approach for neonatal hypoxia-ischemia. Exp Neurol 114450. https://doi.org/10.1016/j.expneurol.2023.114450
- 10. Szrejder M, Typiak M, Pikul P, et al (2023) Role of L-lactate as an energy substrate in primary rat podocytes under physiological and glucose deprivation conditions. Eur J Cell Biol 102:151298. https://doi.org/10.1016/j.ejcb.2023.151298
- 12. Lev-Vachnish Y, Cadury S, Rotter-Maskowitz A, et al (2019) L-Lactate Promotes Adult Hippocampal Neurogenesis. Front Neurosci 13:403. https://doi.org/10.3389/fnins.2019.00403
- 13. Kitaoka Y, Takahashi K, Hatta H (2022) Inhibition of monocarboxylate transporters (MCT) 1 and 4 reduces exercise capacity in mice. Physiol Rep 10:e15457. https://doi.org/10.14814/phy2.15457

- 14. Korol DL, Gardner RS, Tunur T, Gold PE (2019) Involvement of lactate transport in two object recognition tasks that require either the hippocampus or striatum. Behav Neurosci 133:176–187. https://doi.org/10.1037/bne0000304
- Manosalva C, Quiroga J, Hidalgo AI, et al (2021) Role of Lactate in Inflammatory Processes: Friend or Foe. Front Immunol 12:808799. https://doi.org/10.3389/fimmu.2021.808799
- 16. Zhang M, Wang Y, Bai Y, et al (2022) Monocarboxylate Transporter 1 May Benefit Cerebral Ischemia via Facilitating Lactate Transport From Glial Cells to Neurons. Front Neurol 13:781063. https://doi.org/10.3389/fneur.2022.781063
- 17. Kong L, Wang Z, Liang X, et al (2019) Monocarboxylate transporter 1 promotes classical microglial activation and pro-inflammatory effect via 6-phosphofructo-2-kinase/fructose-2, 6-biphosphatase 3. J Neuroinflammation 16:240. https://doi.org/10.1186/s12974-019-1648-4
- 18. Dias C, Fernandes E, Barbosa RM, et al (2023) Astrocytic aerobic glycolysis provides lactate to support neuronal oxidative metabolism in the hippocampus. Biofactors. https://doi.org/10.1002/biof.1951
- Pierre K, Pellerin L, Debernardi R, et al (2000) Cell-specific localization of monocarboxylate transporters, MCT1 and MCT2, in the adult mouse brain revealed by double immunohistochemical labeling and confocal microscopy. Neuroscience 100:617–627. https://doi.org/10.1016/s0306-4522(00)00294-3
- 20. Rafiki A, Boulland JL, Halestrap AP, et al (2003) HIGHLY DIFFERENTIAL EXPRESSION OF THE MONOCARBOXYLATE TRANSPORTERS MCT2 AND MCT4 IN THE DEVELOPING RAT BRAIN. Neuroscience 122:677–688. https://doi.org/10.1016/S0306-4522(03)00654-7
- 21. Pierre K, Pellerin L (2005) Monocarboxylate transporters in the central nervous system: distribution, regulation and function. J Neurochem 94:1–14. https://doi.org/10.1111/j.1471-4159.2005.03168.x
- 22. Magistretti PJ, Allaman I (2018) Lactate in the brain: from metabolic end-product to signalling molecule. Nat Rev Neurosci 19:235–249. https://doi.org/10.1038/nrn.2018.19
- 23. Bittar PG, Charnay Y, Pellerin L, et al (1996) Selective Distribution of Lactate Dehydrogenase Isoenzymes in Neurons and Astrocytes of Human Brain. J Cereb Blood Flow Metab 16:1079–1089. https://doi.org/10.1097/00004647-199611000-00001
- 24. Laughton JD, Bittar P, Charnay Y, et al (2007) Metabolic compartmentalization in the human cortex and hippocampus: evidence for a cell- and region-specific localization of lactate dehydrogenase 5 and pyruvate dehydrogenase. BMC Neurosci 8:35. https://doi.org/10.1186/1471-2202-8-35
- 25. Debernardi R, Pierre K, Lengacher S, et al (2003) Cell-specific expression pattern of monocarboxylate transporters in astrocytes and neurons observed in different mouse brain cortical cell cultures. J Neurosci Res 73:141–155. https://doi.org/10.1002/jnr.10660
- 26. Pellerin L, Magistretti PJ (1994) Glutamate uptake into astrocytes stimulates aerobic glycolysis: a mechanism coupling neuronal activity to glucose utilization. Proc Natl Acad Sci U S A 91:10625–10629. https://doi.org/10.1073/pnas.91.22.10625
- 27. Rosafio K, Castillo X, Hirt L, Pellerin L (2016) Cell-specific modulation of monocarboxylate transporter expression contributes to the metabolic reprograming taking place following cerebral ischemia. Neuroscience 317:108–120. https://doi.org/10.1016/j.neuroscience.2015.12.052
- 28. Zhang Y, Jia P, Wang K, et al (2023) Lactate modulates microglial inflammatory responses after oxygen-glucose deprivation through HIF-1α-mediated inhibition of NF-κB. Brain Res Bull 195:1–13. https://doi.org/10.1016/j.brainresbull.2023.02.002

- 29. Salter MW, Stevens B (2017) Microglia emerge as central players in brain disease. Nat Med 23:1018–1027. https://doi.org/10.1038/nm.4397
- 30. Liddelow SA, Marsh SE, Stevens B (2020) Microglia and Astrocytes in Disease: Dynamic Duo or Partners in Crime? Trends Immunol 41:820–835. https://doi.org/10.1016/j.it.2020.07.006
- 31. Colucci ACM, Tassinari ID, Loss E da S, de Fraga LS (2023) History and Function of the Lactate Receptor GPR81/HCAR1 in the Brain: A Putative Therapeutic Target for the Treatment of Cerebral Ischemia. Neuroscience 526:144–163. https://doi.org/10.1016/j.neuroscience.2023.06.022
- 32. Tassinari ID, de Fraga LS (2022) Potential use of lactate for the treatment of neonatal hypoxic-ischemic encephalopathy. Neural Regeneration Res 17:788–790. https://doi.org/10.4103/1673-5374.322459
- 33. Hoque R, Farooq A, Ghani A, et al (2014) Lactate reduces liver and pancreatic injury in Toll-like receptor- and inflammasome-mediated inflammation via GPR81-mediated suppression of innate immunity. Gastroenterology 146:1763–1774. https://doi.org/10.1053/j.gastro.2014.03.014
- 34. Yang K, Xu J, Fan M, et al (2020) Lactate Suppresses Macrophage Pro-Inflammatory Response to LPS Stimulation by Inhibition of YAP and NF-κB Activation via GPR81-Mediated Signaling. Front Immunol 11:587913. https://doi.org/10.3389/fimmu.2020.587913
- 35. Laroche S, Stil A, Germain P, et al (2021) Participation of L-Lactate and Its Receptor HCAR1/GPR81 in Neurovisual Development. Cells 10:. https://doi.org/10.3390/cells10071640
- 36. Vohra R, Sanz-Morello B, Tams ALM, et al (2022) Prevention of Cell Death by Activation of Hydroxycarboxylic Acid Receptor 1 (GPR81) in Retinal Explants. Cells 11:. https://doi.org/10.3390/cells11132098
- 37. Griego E, Galván EJ (2023) BDNF and Lactate as Modulators of Hippocampal CA3 Network Physiology. Cell Mol Neurobiol 43:4007–4022. https://doi.org/10.1007/s10571-023-01425-6
- 38. Vohra R, Aldana BI, Waagepetersen H, et al (2019) Dual Properties of Lactate in Müller Cells: The Effect of GPR81 Activation. Invest Ophthalmol Vis Sci 60:999–1008. https://doi.org/10.1167/iovs.18-25458
- 39. Herrera-López G, Griego E, Galván EJ (2020) Lactate induces synapse-specific potentiation on CA3 pyramidal cells of rat hippocampus. PLoS One 15:e0242309. https://doi.org/10.1371/journal.pone.0242309
- 40. Scavuzzo CJ, Rakotovao I, Dickson CT (2020) Differential effects of L- and D-lactate on memory encoding and consolidation: Potential role of HCAR1 signaling. Neurobiol Learn Mem 168:107151. https://doi.org/10.1016/j.nlm.2019.107151
- 41. Buscemi L, Price M, Castillo-González J, et al (2022) Lactate Neuroprotection against Transient Ischemic Brain Injury in Mice Appears Independent of HCAR1 Activation. Metabolites 12:. https://doi.org/10.3390/metabo12050465
- 42. Nicola R, Madar R, Okun E (2022) HCAR1-Mediated L-Lactate Signaling Suppresses Microglial Phagocytosis. Neuromolecular Med 24:399–404. https://doi.org/10.1007/s12017-022-08710-5
- 43. Kennedy L, Glesaaen ER, Palibrk V, et al (2022) Lactate receptor HCAR1 regulates neurogenesis and microglia activation after neonatal hypoxia-ischemia. Elife 11:. https://doi.org/10.7554/eLife.76451
- 44. Harun-Or-Rashid M, Inman DM (2018) Reduced AMPK activation and increased HCAR activation drive anti-inflammatory response and neuroprotection in glaucoma. J Neuroinflammation 15:313. https://doi.org/10.1186/s12974-018-1346-7

- 45. Ahmed ME, Selvakumar GP, Kempuraj D, et al (2019) Synergy in Disruption of Mitochondrial Dynamics by Aβ (1-42) and Glia Maturation Factor (GMF) in SH-SY5Y Cells Is Mediated Through Alterations in Fission and Fusion Proteins. Mol Neurobiol 56:6964–6975. https://doi.org/10.1007/s12035-019-1544-z
- M. de-Brito N, Duncan-Moretti J, C. da-Costa H, et al (2020) Aerobic glycolysis is a metabolic requirement to maintain the M2-like polarization of tumor-associated macrophages. Biochimica et Biophysica Acta (BBA) -Molecular Cell Research 1867:118604. https://doi.org/10.1016/j.bbamcr.2019.118604
- 47. Lee S-P, Chao S-C, Huang S-F, et al (2018) Expressional and Functional Characterization of Intracellular pH Regulators and Effects of Ethanol in Human Oral Epidermoid Carcinoma Cells. Cell Physiol Biochem 47:2056–2068. https://doi.org/10.1159/000491473
- 48. Halcrow P, Khan N, Datta G, et al (2019) Importance of measuring endolysosome, cytosolic, and extracellular pH in understanding the pathogenesis of and possible treatments for glioblastoma multiforme. Cancer Rep 2:. https://doi.org/10.1002/cnr2.1193
- 49. Paik S, Somvanshi RK, Kumar U (2019) Somatostatin-Mediated Changes in Microtubule-Associated Proteins and Retinoic Acid-Induced Neurite Outgrowth in SH-SY5Y Cells. J Mol Neurosci 68:120–134. https://doi.org/10.1007/s12031-019-01291-2
- 50. Wölfle U, Haarhaus B, Kersten A, et al (2015) Salicin from Willow Bark can Modulate Neurite Outgrowth in Human Neuroblastoma SH-SY5Y Cells. Phytother Res 29:1494–1500. https://doi.org/10.1002/ptr.5400
- 51. Cruz E, Bessières B, Magistretti P, Alberini CM (2022) Differential role of neuronal glucose and PFKFB3 in memory formation during development. Glia 70:2207–2231. https://doi.org/10.1002/glia.24248
- 52. Schurr A, Payne RS, Miller JJ, Rigor BM (1997) Brain lactate, not glucose, fuels the recovery of synaptic function from hypoxia upon reoxygenation: an in vitro study. Brain Res 744:105–111. https://doi.org/10.1016/s0006-8993(96)01106-7
- 53. Wohnsland S, Bürgers HF, Kuschinsky W, Maurer MH (2010) Neurons and neuronal stem cells survive in glucose-free lactate and in high glucose cell culture medium during normoxia and anoxia. Neurochem Res 35:1635–1642. https://doi.org/10.1007/s11064-010-0224-1
- 54. Monsorno K, Ginggen K, Ivanov A, et al (2023) Loss of microglial MCT4 leads to defective synaptic pruning and anxiety-like behavior in mice. Nat Commun 14:1–18. https://doi.org/10.1038/s41467-023-41502-4
- 55. McKenna MC, Hopkins IB, Carey A (2001) Alpha-cyano-4-hydroxycinnamate decreases both glucose and lactate metabolism in neurons and astrocytes: implications for lactate as an energy substrate for neurons. J Neurosci Res 66:747–754. https://doi.org/10.1002/jnr.10084
- 56. Dovmark TH, Saccomano M, Hulikova A, et al (2017) Connexin-43 channels are a pathway for discharging lactate from glycolytic pancreatic ductal adenocarcinoma cells. Oncogene 36:4538–4550. https://doi.org/10.1038/onc.2017.71
- 57. Sotelo-Hitschfeld T, Niemeyer MI, Mächler P, et al (2015) Channel-Mediated Lactate Release by K+-Stimulated Astrocytes. J Neurosci 35:4168–4178. https://doi.org/10.1523/JNEUROSCI.5036-14.2015
- 58. Descalzi G, Gao V, Steinman MQ, et al (2019) Lactate from astrocytes fuels learning-induced mRNA translation in excitatory and inhibitory neurons. Commun Biol 2:247. https://doi.org/10.1038/s42003-019-0495-2
- 59. Yang J, Yuan S, Jian Y, et al (2023) Aerobic exercise regulates GPR81 signal pathway and mediates complement- microglia axis homeostasis on synaptic protection in the early stage of Alzheimer's disease. Life Sci 122042. https://doi.org/10.1016/j.lfs.2023.122042

- 60. Brooks GA (2020) Lactate as a fulcrum of metabolism. Redox Biol 35:101454. https://doi.org/10.1016/j.redox.2020.101454
- 61. Robergs RA, McNulty CR, Minett GM, et al (2018) Lactate, not Lactic Acid, is Produced by Cellular Cytosolic Energy Catabolism. Physiology 33:10–12
- 62. Blixt J, Song Y, Wanecek M, Gunnarson E (2023) EPO has multiple positive effects on astrocytes in an experimental model of ischemia. Brain Res 1802:148207. https://doi.org/10.1016/j.brainres.2022.148207
- 63. Beppu K, Sasaki T, Tanaka KF, et al (2014) Optogenetic countering of glial acidosis suppresses glial glutamate release and ischemic brain damage. Neuron 81:314–320. https://doi.org/10.1016/j.neuron.2013.11.011
- 64. Gupta P, Hourigan K, Jadhav S, et al (2017) Effect of lactate and pH on mouse pluripotent stem cells: Importance of media analysis. Biochem Eng J 118:25–33. https://doi.org/10.1016/j.bej.2016.11.005
- 65. Li H, Wang Y, Wang B, et al (2021) Baicalin and Geniposide Inhibit Polarization and Inflammatory Injury of OGD/R-Treated Microglia by Suppressing the 5-LOX/LTB4 Pathway. Neurochem Res 46:1844–1858. https://doi.org/10.1007/s11064-021-03305-1
- 66. Qin X, Sun Z-Q, Zhang X-W, et al (2013) TLR4 signaling is involved in the protective effect of propofol in BV2 microglia against OGD/reoxygenation. J Physiol Biochem 69:707–718. https://doi.org/10.1007/s13105-013-0247-6
- Zhang B-J, Men X-J, Lu Z-Q, et al (2013) Splenectomy protects experimental rats from cerebral damage after stroke due to anti-inflammatory effects. Chin Med J 126:2354–2360. https://doi.org/10.3760/cma.j.issn.0366-6999.20122483
- 68. Unsicker C, Cristian F-B, von Hahn M, et al (2021) SHANK2 mutations impair apoptosis, proliferation and neurite outgrowth during early neuronal differentiation in SH-SY5Y cells. Sci Rep 11:2128. https://doi.org/10.1038/s41598-021-81241-4
- 69. Martínez M-A, Rodríguez J-L, Lopez-Torres B, et al (2020) Use of human neuroblastoma SH-SY5Y cells to evaluate glyphosate-induced effects on oxidative stress, neuronal development and cell death signaling pathways. Environ Int 135:105414. https://doi.org/10.1016/j.envint.2019.105414
- 70. Kovalevich J, Langford D (2013) Considerations for the use of SH-SY5Y neuroblastoma cells in neurobiology. Methods Mol Biol 1078:9–21. https://doi.org/10.1007/978-1-62703-640-5_2
- 71. Dravid A, Raos B, Svirskis D, O'Carroll SJ (2021) Optimised techniques for high-throughput screening of differentiated SH-SY5Y cells and application for neurite outgrowth assays. Sci Rep 11:23935. https://doi.org/10.1038/s41598-021-03442-1
- 72. Raghunath M, Patti R, Bannerman P, et al (2000) A novel kinase, AATYK induces and promotes neuronal differentiation in a human neuroblastoma (SH-SY5Y) cell line. Brain Res Mol Brain Res 77:151–162. https://doi.org/10.1016/s0169-328x(00)00048-6
- 73. Al-Chalabi A, Miller CCJ (2003) Neurofilaments and neurological disease. Bioessays 25:346–355. https://doi.org/10.1002/bies.10251
- 74. Gao F, Wu J, Zhou Y, et al (2020) An appropriate ratio of unsaturated fatty acids is the constituent of hickory nut extract for neurite outgrowth in human SH-SY5Y cells. Food Sci Nutr 8:6346–6356. https://doi.org/10.1002/fsn3.1623

- 75. Agrawal PB, Joshi M, Marinakis NS, et al (2014) Expanding the phenotype associated with the NEFL mutation: neuromuscular disease in a family with overlapping myopathic and neurogenic findings. JAMA Neurol 71:1413–1420. https://doi.org/10.1001/jamaneurol.2014.1432
- 76. Hong H, Su J, Zhang Y, et al (2023) A novel role of lactate: Promotion of Akt-dependent elongation of microglial process. Int Immunopharmacol 119:110136. https://doi.org/10.1016/j.intimp.2023.110136
- 77. Li R, Yang Y, Wang H, et al (2023) Lactate and Lactylation in the Brain: Current Progress and Perspectives. Cell Mol Neurobiol. https://doi.org/10.1007/s10571-023-01335-7
- 78. Zhang J, Muri J, Fitzgerald G, et al (2020) Endothelial Lactate Controls Muscle Regeneration from Ischemia by Inducing M2-like Macrophage Polarization. Cell Metab 31:1136-1153.e7. https://doi.org/10.1016/j.cmet.2020.05.004
- 79. Chaudhari P, Madaan A, Rivera JC, et al (2022) Neuronal GPR81 regulates developmental brain angiogenesis and promotes brain recovery after a hypoxic ischemic insult. J Cereb Blood Flow Metab 42:1294–1308. https://doi.org/10.1177/0271678X221077499
- 80. Lauritzen KH, Morland C, Puchades M, et al (2014) Lactate receptor sites link neurotransmission, neurovascular coupling, and brain energy metabolism. Cereb Cortex 24:2784–2795. https://doi.org/10.1093/cercor/bht136
- 81. Morland C, Lauritzen KH, Puchades M, et al (2015) The lactate receptor, G-protein-coupled receptor 81/hydroxycarboxylic acid receptor 1: Expression and action in brain. J Neurosci Res 93:1045–1055. https://doi.org/10.1002/jnr.23593

Statements & Declarations

Funding:

This study was supported by Conselho Nacional de Desenvolvimento Científico e Tecnológico (CNPq), Coordenação de Aperfeiçoamento de Pessoal de Nível Superior (CAPES), National Institute of Science and Technology on Neuroimmunomodulation (INCT-NIM), FIOCRUZ Institutional Internationalization Program (CAPES/PrInt-Fiocruz), UFRGS Institutional Internationalization Program (CAPES/PrInt-UFRGS), and Erasmus+ Funding Programme.

Competing interests:

The authors declare no competing interests.

Authors' contributions:

Conceived and designed the experiments: IDT, DAMC, RPG, AHP, VBJ and LSF. Performed the experiments: IDT and FSR. Analyzed the data: IDT, FSR, VBJ, and LSF. Data interpretation: IDT, DAMC, RPG, AHP, and LSF. Wrote the first draft of the manuscript: IDT, LSF. Revised critically the manuscript: CB, DAMC, RPG, and AHP. Grammar review: CB. All authors reviewed the final version of the manuscript.

Data Availability:

Data are available upon reasonable request.

Ethics approval:

Institutional ethical approval was not required, as the present study used only cell lines, and live animals were not used in the experiments.

Consent to participate:

Not applicable.

Consent to publish:

Not applicable.